

UCRL-JC-130951

PREPRINT

# Modeling of Laser Produced Plasma and Z-Pinch X-Ray Lasers

A. L. Osterheld, V. Shlyaptsev, J. Dunn, J. J. Rocca, M. C. Marconi,  
C. H. Moreno, J. J. Gonzales, M. Frati, P. V. Nickles,  
M. P. Kalashnikov, W. Sandner

This paper was prepared for submittal to the  
6th International Conference on X-Ray Lasers  
Kyoto, Japan  
August 31-September 4, 1998

February 7, 1999



This is a preprint of a paper intended for publication in a journal or proceedings.  
Since changes may be made before publication, this preprint is made available with  
the understanding that it will not be cited or reproduced without the permission of the  
author.

#### DISCLAIMER

This document was prepared as an account of work sponsored by an agency of the United States Government. Neither the United States Government nor the University of California nor any of their employees, makes any warranty, express or implied, or assumes any legal liability or responsibility for the accuracy, completeness, or usefulness of any information, apparatus, product, or process disclosed, or represents that its use would not infringe privately owned rights. Reference herein to any specific commercial product, process, or service by trade name, trademark, manufacturer, or otherwise, does not necessarily constitute or imply its endorsement, recommendation, or favoring by the United States Government or the University of California. The views and opinions of authors expressed herein do not necessarily state or reflect those of the United States Government or the University of California, and shall not be used for advertising or product endorsement purposes.

# Modeling of Laser Produced Plasma and Z-Pinch X-Ray Lasers

**A.L.Osterheld, V.Shlyaptsev<sup>1</sup>, J.Dunn,**

Lawrence Livermore National Laboratory, Livermore, CA 94550

**J.J.Rocca, M.C. Marconi, C.H.Moreno, J.J.Gonzales, M.Frati,**

Colorado State University, Fort Collins CO, 80523

**P.V.Nickles, M.P.Kalashnikov, W. Sandner,**

Max-Born Institute, Berlin

**Abstract.** In this work we describe our theoretical activities in two directions of interest. First, we discuss progress in modeling laser produced plasmas mostly related to transient collisional excitation scheme experiments with Ne- and recently with Ni-like ions. Calculations related to the delay between laser pulses, transient gain duration and hybrid laser/capillary approach are described in more detail.

Second, the capillary discharge plasma research, extended to wider range of currents and rise-times has been outlined. We have systematically evaluated the major plasma and atomic kinetic properties by comparing near- and far-field X-ray laser output with that for the capillary Argon X-ray laser operating under typical current values. Consistent with the experiment insight was obtained for the 469Å X-ray laser shadowgraphy experiments with very small kiloamp currents. At higher currents, as much as ~200 kA we evaluated plasma temperature, density and compared x-ray source size and emitted spectra.

## Introduction

Since the previous conference on X-ray lasers in Lund [1] our activities have been mostly concentrated on collisional excitation X-ray lasers created by high power chirped pulse amplification (CPA) lasers and Z-pinch electrical discharges. With laser produced plasmas the main attention has been devoted to transient collisional excitation X-ray lasers. Following this approach, laser action in several elements at wavelengths of 100-300 Å as well as the intensity saturation was achieved recently [2-8]. Comparison with numerous experiments at LLNL [4, 6-9] and at different groups in the world [2,10,11] was performed for a better understanding of transient inversion phenomena.

Another approach for table-top X-ray lasers is one of the modifications of Z-pinch, i.e. fast capillary discharge (FCD) [12,13]. Like other Z-pinch, FCDs remain to be difficult objects for calculations. For their modeling RADEX also incorporates self-consistent magnetic hydrodynamics, material ablation and ionization from capillary walls, as well as non-LTE atomic physics and radiation transport in thousands of emission lines. In fact, the use of knowledge obtained in laser plasma modeling and experiments

substantially facilitates and improves the reliability of numerical description of these discharges.

Numerical models of RADEX designed for investigating both laser and Z-pinch plasmas, cover the main aspects of plasma formation, fully transient atomic kinetics, radiation transport and dynamics of X-ray signal amplification in a refracting and rapidly changing laser medium. Due to the complexity of the X-ray laser problem, satisfactory explanation of real situations or prediction of correct values of input and output parameters of laser-target interaction (including laser fluxes/currents, ns-ps laser delays, energy requirements, space-time gain evolution, intensity saturation) require comparison with the experiments. The measured X-ray laser parameters were well reproduced numerically allowing in turn further improvement of the RADEX code physical model. This continually requires improvement of physics, code structure and performance. Besides the purely numerical problem of large-scale code integration and implementation on more advanced SMP-ready OS, the major modifications of the physical model were in the atomic physics of overheated plasma, improvement of ray-tracing routines and extending ranges of validity and applicability with capillary plasma. It includes more accurate inner-shell ionization model which revealed that this atomic process becomes dominant for ionization of overheated plasma of pre-Ni-like ions as well as influencing kinetics of Ni-like ions themselves. Amplification dynamics model includes photon on-the-fly interaction with rapidly evolving in space and time active medium defined by transient atomic processes and hydrodynamics.

## **I. Laser Produced Plasma**

After demonstration of transient collisional excitation approach [11] the comprehensive characterization and development in several different directions have been performed both experimentally and numerically. First, utilizing the high-energy picosecond facility at RAL the output of transient X-ray lasers based on Ne-like ions (Ti at 326 Å nm and Ge at 196 Å) was optimized by changing irradiation conditions in a broad range of flux densities. The ~1 ns prepulse for Ti plasma for example was scanned from 0.25 J to 20 J with optimum for given line focus width and ns-ps pulse delay (100 μm and 1 ns, respectively) on the level of 3-5 J with definite lasing starting from 0.25 J. The ~3 ps main pulse energies were also widely varied up to maximum allowed by the Vulcan-CPA system, 20 J for Ti and up to 40 J for Ge [2, 3]. Then, the X-ray laser saturation intensity was achieved for Ti and appropriately higher values for higher-Z Ge. The optimization experiments for shorter length and lower energy conditions showed that saturation for Ti can be achieved by lowering the energy to very moderate table-top energies, as low as ~5 J. The gain in the range of very high values ~45 cm<sup>-1</sup> was demonstrated on 326 Å 3p-3s transitions and ~35 cm<sup>-1</sup> on 301 Å 3d-3p transitions. Finally, the angular characteristics of these lasers, divergence and deflection from axial direction, have been also measured at RAL [2].

Research of Ne-like ions at LLNL have been performed on a small-scale facility of a different design and was concentrated on some other aspects of lasing. Here besides Ti and V, the element Fe [14] was shown to lase successfully. Then with just ~5 Joules in both ~0.8 ns and ~1 ps pulses large jump in lasing wavelength to 147 Å and with GL~12.5 was achieved utilizing Ni-like ions Pd (Z=46) [4]. Also strong output was measured for the 4d-4p J=0-1 line in lower Z Ni-like ion sequence from Y (Z=39) to Mo (Z=42), lasing from ~190 Å to 240 Å was measured by pumping with less than 5 J total energy on target [8]. It is

important to note that in quasi-steady state approximation low  $Z$  elements  $Z < 42$  do not have inversion in the under dense plasma where  $n_e > 10^{19} \text{ cm}^{-3}$  interested for effective absorption of  $1\omega$  laser. This is because the radiative probability from the lower laser level to ground state is not substantially larger than one between excited states together with their collisional mixing. Additionally reabsorption and cascades further quench the inversion. Hence, in spite of attractively small requirements for laser energy, achievement of pronounceable lasing on these elements with relatively long pulsed lasers [15] is problematic. In transient collisional scheme these elements, as usual, demonstrate very high gain, but due to known decreased inversion life-time compared to heavier elements [16], the intensity saturation here is harder to reach. This question will be addressed in future experiments with traveling wave excitation.

### 1.1 Optimal delay between ns and ps laser pulses

An understanding of how to set an optimal long pulse-to-short pulse delay is one of the important questions needing to be answered for effective laser operation in the transient regime. This issue was known theoretically since it represents one of the basic ways of transient scheme implementation using two sequential laser pulses, but it was not investigated systematically. It was found experimentally in the works of other groups with Ne-like Ti x-ray laser plasmas that lasing action had a maximum intensity if the two pulses were separated by between one and two nanoseconds [11]. This question was investigated in the current experiments at LLNL. It should be noted that there exists a similarity between this scheme and previous experiments with pre-pulse formed x-ray laser plasmas in the quasi-steady state regime. It was found in many experiments (see for example [17]), that the QSS lasing could be maximized with different kinds of low density pre-pulses, multiple pulses of different duration, with optimized energies and delays. The purpose of the prepulse was to substantially reduce refraction effects. With the transient excitation scheme the function of the prepulse is different and hence the methods of optimization are different from the previous QSS approach. Pre-formation of plasma by the prepulse in the transient scheme not

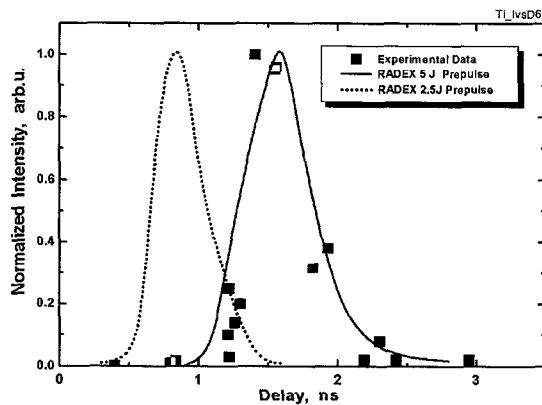


Fig.1. Ti 326A X-ray laser intensity vs long-short pulse delay. Absolute intensity with 2.5J prepulse  $\sim 3$  times larger than with 5J.

only solves the problem of refraction but also of equal importance prepares the active ions participating in the amplification and plasma with required parameters. A number of experiments and comparisons with RADEX simulations have been made for different atomic elements. Fig.1 (solid curve) shows the intensity of Ne-like Ti 3p-3s  $J=0-1$  laser at 326 Å as a function of delay introduced for the short pulse relative to the peak of the 800 ps plasma forming pulse. It can be seen, that lasing does not occur if the picosecond pulse arrives earlier than 1.0 – 1.2 ns after the long pulse. There

is a window where good lasing is observed, centered at  $\sim 1.5$ - $1.6$  ns, followed by a fast decrease for delays of more than 2.2 ns. In general, this behavior at smaller delay is more than just the influence of refraction effects at the beginning of expansion. This is confirmed in the simulations by artificially reducing the effects of refraction by an order of magnitude: though absolute intensity is increased, the time of optimal delay and width of lasing window remain relatively unchanged. Another confirmation is X-ray laser signal with a factor of two reduction in the nanosecond laser energy (dotted line on Fig.1). Despite density profiles at the same delays remaining almost the same in these two cases, the optimal time is shifted to earlier moments when gradients and refraction are larger. This last example is a typical case

where *a-priori* estimations or hydro/kinetics modeling without including ray-tracing amplification dynamics will probably be inconclusive or inaccurate.

First, the reason lasing does not appear prior to a specific moment lies in the physics of the transient inversion. To achieve substantial transient gain, the initial plasma temperature before the picosecond temperature jump must be low enough to empty the excited level populations. After the 800 ps prepulse has finished, the laser plasma is allowed to cool down by expansion and radiation to reach less than 80 eV for Ti and less than 90 eV for Pd. Unless these conditions are achieved the transient gain is small. Additionally, and perhaps crucially, the reason for this particular

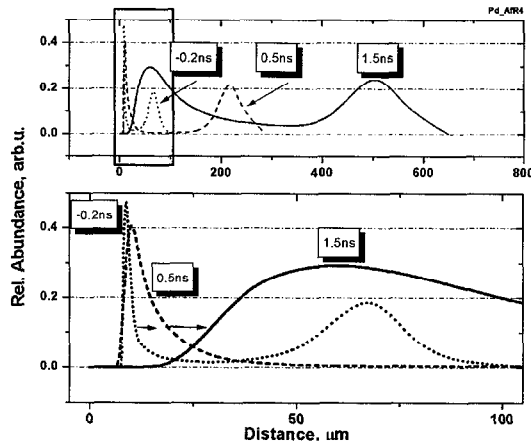


Fig.2 Profiles of relative abundance of Ni-like Pd (lower graph is selected and magnified part of upper one). Profiles correspond to three moments with respect to the maximum intensity of 800 ps laser pulse, while ps-pulse is off.

delay for the given laser parameters (qualitatively similar to both Ne-like Ti and Ni-like Pd, which have similar ionization potentials) is related to the specific ionization balance achieved during the pre-pulse shown in Fig.2 for Ni-like Pd. With 5 J or more in pre-pulse all sub-critical low density corona is over-ionized relative to Ne/Ni-like ions. In the above-critical part of corona there always exists a layer where Ne- and F-like ions or Ni- and Co-like are present as the high abundance species. During the next  $\sim 1.5$  ns before the ps-pulse arrives, this dense layer expands by widening to  $100 \mu\text{m}$  rarefying to  $10^{20} \text{ cm}^{-3}$  and cooling to under 80 eV. The plasma ion charge remains relatively frozen keeping the Ne-like or Ni-like ions in substantial abundance. The fall in XRL intensity for large delays is due to further motion of the lasing ion cluster, substantial plasma expansion and the resultant drop in the density. This causes in turn a decrease in the short pulse laser absorption and hence reduced gain-sensitive plasma temperatures during the short pulse. At these late delays the density and corresponding gradients are reduced by more than 50% which is beneficial for refraction effects but is not sufficient to compensate for the lower gain coefficient. In summary, this particular case with noted laser parameters, simply reflects the fact that with 5-6 J in the prepulse all sub-critical plasma is overionized with respect to the lasing ions. Specific  $\sim 1.6$  ns delay in this situation is defined by speed of expansion of proper internal layer. Calculations

in turn suggest that optimum prepulse energy lies nearer  $\sim 2\text{J}$  with an appropriately smaller delay  $\sim 0.5\text{-}1\text{ ns}$ . This is because the larger relative abundances of working ions are created at the low density corona (and not in overcritical layer which then recombine) with refraction effects still remaining low.

### ***1.2 Duration of the Transient Inversion in Ni-like Pd***

We estimated [9] the gain lifetime of the  $147\text{ \AA}$  Ni-like Pd X-ray laser produced by an  $800\text{ps}$ ,  $1\text{ TW cm}^{-2}$  formation pulse and a  $1.1\text{ ps}$ ,  $800\text{ TW cm}^{-2}$  pump pulse from the experiment intensity versus length data. A  $1/e$  effective transient gain lifetime of approximately  $7\text{-}8\text{ ps}$  is determined and compared with RADEX simulations of numerical  $1/e$  effective gain lifetime obtained similarly from intensity versus length calculations. The faster effective gain decay of  $\sim 7\text{ps}$  occurs early in time and corresponds to the transient high gain regime. The second has a slower effective gain decaying with  $\sim 18\text{-}20\text{ps}$  at about  $25\text{ - }30\text{ps}$  after the short pulse deposition when gain is already close to quasi-steady state value of  $\sim 4\text{cm}^{-1}$ . The inferred maximal values of the gain and its duration correspond to the optimal electron densities Pd X-ray laser operates of  $1\text{ - }1.5 \times 10^{20}\text{ cm}^{-3}$ . The equivalent propagation time would correspond to a target length of approximately  $0.2\text{ cm}$  (see further detail in [9]). Higher effective gains are expected with traveling wave irradiation geometry to synchronize the phase of the pump pulse with the propagation of the x-ray laser along the plasma column (as shown in [5]).

### ***1.3 Intensity Saturation of Transient X-ray Laser on Ne-like Titanium***

In the experiments [2] with  $\sim 20\text{ J}$  in ns-duration plasma formation and ps driving pulses, the saturation intensity was achieved on Ti  $326\text{ \AA}$  and similarly repeated for  $20\text{ - }40\text{ J}$  on Ge at  $196\text{ \AA}$  [3,18]. As well as high  $GL \sim 16.7$  and high x-ray laser intensity which surpassed the saturation limit, one more property of Ne-like Ti associated with its atomic kinetics allowed us to reliably determine gain saturation. This was the intensity behavior of another Ne-like Ti line,  $301\text{ \AA}$   $3d\text{-}3p$  transition, which increases close to saturation too. This line was first discovered as a curious exception in QSS [19] since its lower level was not directly depopulated to the ground state, while the upper state depends on optical thickness in the  $3d\text{-}2p$  resonance line. It showed a smaller but noticeable gain in optically thick plasma reported in several works in QSS and also in transient case (see refs in [2, 20]). This line may serve as a supplemental diagnostics tool of saturation on the  $3p\text{-}3s$  line if the  $3d\text{-}3p$  line intensity surpasses the former. This is a result of  $\sim 2.5$  times higher saturation intensity associated with a larger linewidth (see details in [2]).

## **II. Capillary Discharge Plasmas**

One of our recent numerical and experimental works on capillary discharge plasmas was the systematic investigation of lasing dynamics utilizing near- and far-field imaging techniques [21]. FCD X-ray lasers operating in Ne-like Argon at  $469\text{ \AA}$  have already demonstrated high efficiency, saturated operation and table-top dimensions. Novel

approaches to X-ray lasers in capillary discharge Z-pinches have been associated with achievement of higher currents or shorter current risetimes. First results with  $\sim 200\text{kA}$  current and  $\sim 10\text{ns}$  duration have been reported in [22,29]. Heading in the direction of capillary discharges with lower currents or longer durations may have limited applications to generating x-ray lasers, but could provide supplemental benefits when combined with other methods. One of the most promising approaches we discuss here is the utilization of the advantages of capillary Z-pinch plasma formation (including very high almost 1-D symmetry of contraction, self-focusing properties, simplicity and efficiency) with the possibility of transient inversion by ultrashort lasers [23]. We will shortly give an overview of the results obtained in these three directions.

### 2.1 Near- and Far-Field Beam Divergence of Capillary X-ray Laser

In capillary discharge the fast current pulse rapidly compresses the plasma to form a needle-shaped column in which lasing is obtained by collisional electron excitation of the ions [12,13]. Recently, two dimensional near field imaging studies of laser pumped soft x-ray amplifiers have been reported [24-27]. Significant insight into the physics of this new kind of soft x-ray amplifier can be gained from such images. Knowledge of the near field and far-field spatial distribution of the output of these lasers is of both practical and basic interest.

The experiments [21] showed that refraction is responsible for increasing the size and divergence of the beam from about  $150$  to  $300\mu\text{m}$  at the exit of the amplifier and from  $2$  to

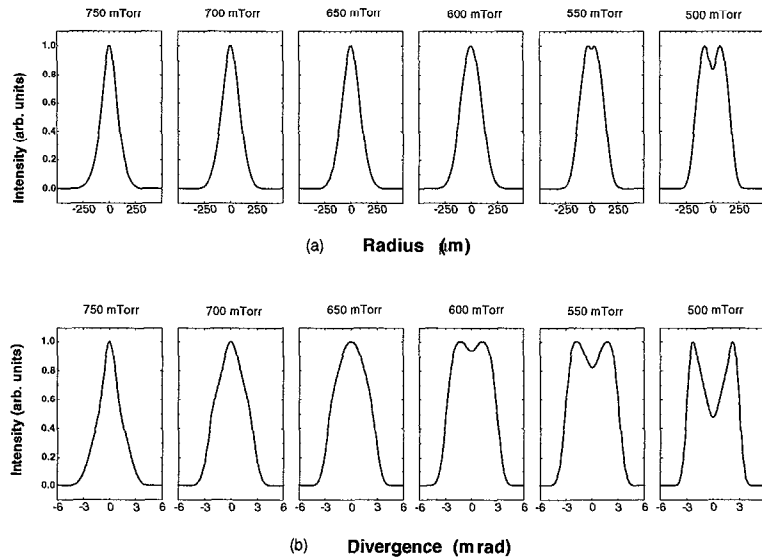


Fig.3 Near- (a) and Far- (b) field intensity profiles calculated by RADEX for capillary X-ray laser at the pressures indicated on top

5 mrad respectively as the discharge pressure is decreased from 750 to 500 mTorr, in good accordance with the calculations. The RADEX results show that beam refraction and the gain coefficient both increase as the pressure is reduced. The former is mostly due to reduced



plasma size, while the latter is a consequence of larger temperatures, higher optimum densities, and reduced opacity at the time of lasing. Refraction was found to strongly influence the intensity behavior of this capillary discharge laser and its near- and far-field profiles. This was already known to be the case in laser driven soft X-ray lasers with much higher electron densities but shorter plasma columns. Quantitative comparison of these cross-sections with experimental observations show in general good agreement between the results of the model and the experiment. The model clearly reproduces the experimentally observed evolution of the laser output from a low divergence beam with a single peak profile at a pressure of 750 mTorr into a larger divergence beam with a ring structure at lower pressures (Fig.3) (see in full detail [21]). This is also a good example which shows the complex influence of pressure, current and other parameters on X-ray laser near-field and far-field images and output intensity. The dominant processes responsible for near- and far-field image formation is hard to select based on *a-priori* estimations or experiment alone until the X-ray laser characteristics were completely reproduced in numerical simulations trials.

## 2.2 Modeling of High-Current Electrical Discharge.

The observation of large soft x-ray amplification in the plasma of a capillary discharge and the subsequent demonstration of a saturated discharge pumped table-top soft x-ray laser in Ne-like Ar at 469 Å have established a new approach for the development of compact and practical soft x-ray lasers. The possibility of achieving higher temperatures and densities with such techniques is the next step in this field. In references [22, 29], recent experiments have been presented with higher current drives showing spectra and pinhole images of the compressing plasma obtained with an Argon filled capillary. Calculations of hydrodynamics, ionization and radiation obtained with driver parameters suggest that the maximum obtained ion charge, plasma dimension and time evolution are in general agreement with this data. Most

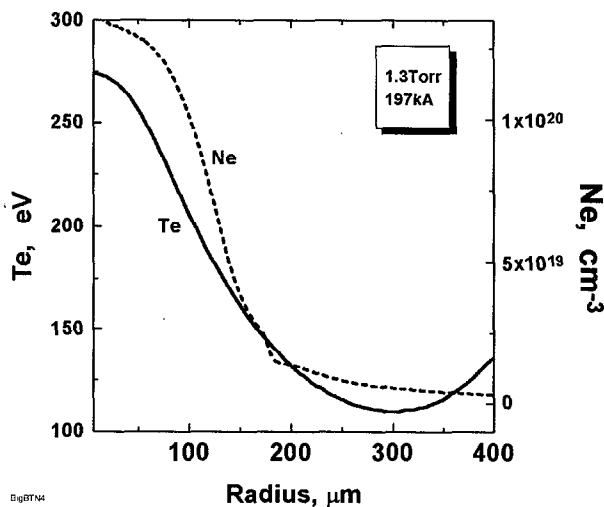


Fig.4 Electron temperature and density profiles of Argon-filled capillary at 1.3Torr 197kA

importantly, the temperature approached 200-275 eV and was 3-4 times larger than obtained with previous experiments at 35-40 kA current drives. This value is larger than the ionization temperature for steady-state ionization balance because of the short life-time of the compressed core compared to the ionization time of high-Z ions. The speed of accelerated plasma sheath before the collapse reaches  $1.5 \times 10^7$  cm/s. The final diameter of density profile and maximum density are 250-300  $\mu\text{m}$  and  $1 \times 10^{20} \text{ cm}^{-3}$ , respectively, which is also ~2-3 times larger than was obtained previously. With such hydro and ionization parameters due to

increased current densities, radiation and ionization losses, the behavior of high-Z plasmas tends to become unstable. Since this is important for many future applications including X-ray laser development, further investigations will be conducted to find out if this really happen and in what extent 1D approach remains to be adequate.

### 2.3 Plasma Dynamics of Small Current Capillary Discharge

We performed the numerical modeling of shadowgraphy experiments [28] made with 469 Å X-ray laser which irradiated capillaries driven by small currents of the order of several kiloamps. Calculations revealed many new interesting properties of capillary discharges. The spectra of the micro-capillary plasma shows emission from carbon ions ranging from CII to CIV and from oxygen ionized up to OVI [28]. In the initial moments of the pinch evolution, when the current is particularly small, unusually high ionization was observed in agreement with simulations. These conditions last for approximately 10 - 20 ns. During the current maximum at ~70ns, the central region becomes hot again with a temperature of ~15 eV, which is high enough to ionize carbon and oxygen species ablated from the walls to the above noted states. When the density (see Fig.4 where density values are close to plastic capillary) and reabsorption in atomic lines increase with time, photoionization from excited states as well as from the ground states of higher Z ions contributes to the absorption of probing Argon X-ray laser 469 Å radiation. Importantly for X-ray lasers, the calculations also show that the electron density, which increases with time above  $2 \times 10^{19} \text{ cm}^{-3}$  at the center of the capillary, has a concave profile with a minimum on axis.

### III. Hybrid X-ray Laser Approach

Although it is very difficult to achieve transient inversion timescales with Z-pinches there

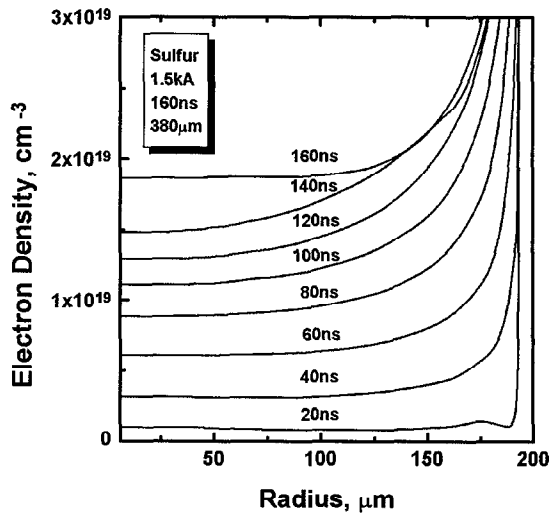


Fig. 5 Electron density profiles of evacuated capillary at different moments starting from beginning of 1.5ns 160ns (base) current pulse.

are still some unique properties of capillary discharges that can be utilized for x-ray lasers. In [23] it was proposed that the combination of short pulse laser-heating with a capillary type pre-formed plasma could realize the benefits from each scheme. To evaluate these new approaches a new more detailed model for hollow evacuated capillaries was incorporated into RADEX. Fig. 5 shows the calculated electron density profiles for a sulfur capillary driven by a 1.5 kA, 160 ns duration current pulse. Though not absolutely necessary, the current can be increased relatively easily to several kiloamps, so that the temperature can be extended

to 30 - 40 eV. Ne-like ions are then substantially abundant in the plasma while the fraction can also be further increased by heating from the picosecond laser pulse. As shown in Fig. 5, the nominal density in the capillary center increases to higher values by waiting later during the decay in the current pulse cycle. It can be seen that the electron density profile in this design is concave, hence the index of refraction is convex, and the radius of curvature changes with time. Therefore, by selecting the appropriate arrival time of the short laser pulse, the optimum electron density for the transient excitation can be chosen. It should be noted that the transient collisional excitation scheme operates at any density and is not destroyed by re-absorption effects. The curvature of the density profile is smaller near the current minimum at 160 ns. This continues later in time when the plasma starts to escape from the ends of the capillary.

This concept and choice of the optimal moment for the laser heating has a number of advantages for x-ray lasers. In addition to the traveling wave propagation of the laser pulse, the tailored density profile allows waveguiding of the amplified x-ray photons and longer propagation lengths in the gain region. Calculations suggest that with this technique lasing for Ne-like sulfur may be achieved with picosecond laser energy of 0.25 - 1 J or lower. The required electron temperature for lasing is in the range of 100 - 150 eV and transient gains can be as high as 20 - 50 cm<sup>-1</sup> depending on the initial density.

A similar approach utilizing wave-guiding properties of microcapillaries filled with laser pre-formed plasma has been successfully developed at Princeton [30]. Our modeling shows that with capillary discharges it is possible to control the refractive and absorption properties as well as the plasma pre-heating required for x-ray laser experiments.

**Acknowledgements:** We thank M. Eckart for continued support. One of us (V.N.S.) acknowledges also support from Yu.V.Afanasiev, N.G.Basov and V.A.Isakov of Lebedev Physical Institute and H. Baldi of ILSA. The work of V.N.S., A.L.O. and J.D. was performed under the auspices of the US Department of Energy by Lawrence Livermore National Laboratory under contract W-7405-Eng-48. Part of this work was supported by NSF-DOE grant ECS-9713297 and by NSF grant DMR-9512282.

<sup>1</sup> Also UC Davis / ILSA. E-mail: [shlyaptsev1@llnl.gov](mailto:shlyaptsev1@llnl.gov), [slava@lamar.colostate.edu](mailto:slava@lamar.colostate.edu)

## References

1. "X-ray Lasers 1996", Proc. of the 5<sup>th</sup> Int. Conf. on X-ray Lasers, Lund, Sweden, 10-14 June 1996, IOP, vol. **151**.
2. Kalachnikov M.P., Nickles P.V., Schnurer M., Sandner W., Shlyaptsev V.N., Danson C., Neely D., Wolfrum E., Zhang J., Behjat A., Demir A., Tallents G.J., Warwick P.J., Lewis C.L.S. 1998, *Physical Review A*, **57**, no.6, p.4778-83.
3. Warwick P J, Lewis C L S, Kalashnikov M P, Nickles P V, Schnurer M 1998 *JOSA B* **15**(6) 1808.
4. Dunn J, Osterheld A L, Shepherd R, White W E, Shlyaptsev V N, Stewart R.E 1998 *Phys.Rev.Lett.* **80**, p.2825.
5. Klisnick A et al, this Proc; Nickles P V et al, this Proc.
6. Dunn J, Shlyaptsev V N, Osterheld A L, White W E, Shepherd R, Stewart R E 1998 LLNL Report UCRL-JC-131413

7. Dunn J, Shlyaptsev V N, Osterheld A L, White W E, Shepherd R, Stewart R E 1998 LLNL Report Number UCRL-JC-131413
8. Dunn J, Li Y, Nilsen J, Osterheld A L, Shlyaptsev V N 1998 to be published in Optics Letters, LLNL report UCRL-JC-132041
9. Osterheld A L, Dunn J, Shlyaptsev V N, these Proc.
10. Nickles P V, Shlyaptsev V N, Schnurer M, Kalachnikov M, Schlegel T, Sandner W 1997 Optics Communications, **142**, p.257-61
11. Nickles P V, Shlyaptsev V N, Kalachnikov M, Schnurer M, Will I, Sandner W 1997 Physical Review Letters, **78** (14), p.2748-51
12. Rocca J J, Shlyaptsev V N, Tomasel F G, Cortazar O D, Hartshorn D and Chilla J L A 1994 Phys. Rev. Lett. **73**, 2192
13. Rocca J J, Clark D P, Chilla J L A, and Shlyaptsev V N 1996. Phys. Rev. Lett, **77**, 1476
14. Dunn J et al These Proc.
15. Basu S, Hagelstein P, Goodberlet J G, Muendel M H, and Kaushik S 1993 Appl. Phys. B **57**, 303.
16. Afanasiev Yu V and Shlyaptsev VN 1989, Sov. J. Quantum Electron. **19**, 1606
17. Nilsen J, MacGowan B.J., Da Silva L.B., and J.C. Moreno, 1993 *Phys. Rev. A* **48** (6), 4682; Fill E E, Li Y, Pretzler G, Schlögl D, Steingruber J, Nilsen J 1995, *Physica Scripta* **52**, 158
18. Healy B, Janulewicz K A, Plowes J A, Pert G J 1996 Opt. Commun. **132**, 442.
19. Vinogradov A V and Shlyaptsev VN 1983 Sov. J. Quantum Electron., **13**, 303.
20. Nilsen J These Proc.
21. Moreno C H, Marconi M C, Shlyaptsev V N, Benware B R, Macchietto C D, Chilla JLA, Rocca J J, Osterheld A L 1998 *Physical Review A* **58**(2), p.1509
22. Rocca J J et al These Proc.
23. Shlyaptsev V N, Rocca J J, Kalashnikov M P, Nickles P V, Sandner W, Osterheld A L, Dunn J, Eder D C 1997 Proc of SPIE **3156**, 193
24. Moreno J C, Nilsen J, Li Y L, Lu P X and Fill E E 1996. Opt. Lett. **21**, 866
25. Nilsen J, Moreno J C, Da Silva L B and Barbee T W 1997 Jr. Phys. Rev. A **55**, 827
26. Nilsen J, Zhang J, MacPhee A G, Lin J, Barbee T W et al 1997 Phys. Rev. A **56** 3161
27. Zhang J, Warwick J, Wolfrum E et al 1996 Phys. Rev. A **54**, 4653
28. Moreno C H, Marconi M C, Shlyaptsev V N, and Rocca J J 1998 IEEE Trans on Plasma Sci
29. Gonzales J J et al These Proc.
30. Korobkin D, Goltsov A, Morozov A, Suckewer S 1998 Phys.Rev.Lett. **81**, p.1607